MicroDoppler Signatures of Anomalies in Human Gait

Shobha Sundar Ram[1], Hao Ling[2]

Dept. of Electrical and Computer Engineering, University of Texas at Austin
1 University Station, Austin, TX 78712 USA

[1]shobhasram@mail.utexas.edu

[2]ling@ece.utexas.edu

***Abstract*— Joint time-frequency representations of the radar return from human motions show interesting microDoppler features due to the movements of the human limbs. We examine the microDoppler signatures of some anomalies in the human gait patterns, such as walking while holding an object. This is carried out by comparing the anomalous gait signatures with that from normal gait. Both simulated and measured microDoppler data are presented.**

***Keywords*: microDoppler, human, gait, short-time Fourier transform**

I. INTRODUCTION

There has been a great deal of interest recently in developing Doppler radars for detecting, tracking and monitoring human activities in non-line-of-sight environments for security and surveillance applications [1]-[6]. Moving humans are easily detectable by Doppler radar since stationary background clutters commonly encountered in urban settings can be largely suppressed. Microwave frequencies below 5GHz are capable of penetrating through most wall materials [7]. Most importantly, a human is a non-rigid body, and the swinging movements of the human arms and legs give rise to interesting "microDoppler" features [8], [9]. When the Doppler returns are viewed in the joint time-frequency space, the time-varying microDoppler features from different moving parts of the human can provide revealing information about the types of human motion. MicroDoppler signatures have been exploited for identification and classification of different human motions [2],[3],[10]. Recent simulation and measurement studies have also suggested that even complex inhomogeneous walls do not significantly distort the microDoppler returns of a moving object behind a wall, making them rather robust features [11]. In this work, we examine human microDoppler signatures due to anomalies in human gait patterns, such as walking while holding an object. MicroDoppler data are generated from both electromagnetic simulation and laboratory measurement.

II. SIMULATED SPECTROGRAMS OF REGULAR AND ANOMALOUS HUMAN GAIT PATTERNS

In [12], we proposed a method for simulating the Doppler spectrograms of different human motions described by computer animation data. The scattered returns from a human are simulated using the primitive based prediction technique proposed in [13]. Different parts of the human body are modeled as simple primitive shapes such as spheres and ellipsoids, whose radar cross sections (RCS) are well characterized [14]. The dielectric property of human flesh [15] is also incorporated in the computation of the RCS. The human Doppler returns are generated from the complex sum of the returns of all the body parts. It is noted that this approach ignores the possible mutual shadowing of the body parts, as well as any higher-order interactions among the body parts.

We first simulate the Doppler spectrogram of a normal human gait pattern. The animation data is obtained from ACCAD Motion Capture Lab from Ohio State University. The human walks from (-7,1,7)m to (-3,1,3)m over a duration of 3s and the radar is assumed to be located at (0,1,0)m. The Doppler returns are simulated for a carrier frequency of 12GHz. The time-varying Doppler returns are processed with the short-time Fourier transform (STFT) with a dwell time of 0.1s and the resulting spectrogram, $\chi_{regular}(t,f)$, is shown in Fig. 1a. Here, strong returns at 120Hz arise from the motion of the torso of the human. The periodic features arise from the movements of the arms and legs of the human. The motion of the legs gives rise to the highest Dopplers. This is followed by the motion of the arms. Fig. 1b, shows the Doppler spectrogram, $\chi_{anomalous1}(t,f)$, of a human walking without swinging his arms. All the microDoppler features observed in Fig. 1a are again observed in this figure except for the microDoppler from the arms. Fig. 1c, shows the Doppler spectrogram, $\chi_{anomalous2}(t,f)$, of a man carrying a 1.1m long stick in his left hand (Fig. 1d). The stick is modeled as a metal cylinder, whose RCS is again well characterized [16].

A simple way to deduce the presence of anomalies in the human gait is to compare the spectrograms of the anomalous human gaits $\chi_{anomalous1,2}(t,f)$ with the regular human gait, $\chi_{regular}(t,f)$, spectrogram. This is carried out by generating two types of difference maps: (1): $\chi_{regular}(t,f) - \chi_{anomalous1}(t,f)$ and (2): $\chi_{anomalous2}(t,f) - \chi_{regular}(t,f)$. The first map is generated by subtracting the spectrogram in Fig. 1b from Fig. 1a in the decibel scale. The resulting spectrogram in Fig. 1e indicates that the microDoppler features corresponding to the movements of the arms are absent in $\chi_{anomalous1}(t,f)$. The second

map, Fig. 1f, is generated by subtracting the spectrogram in Fig. 1a from Fig. 1c. It shows the additional microDoppler feature present in $\chi_{anomalous2}(t,f)$, which arises from the motion of the metal stick. Thus microDoppler features arising from anomalies in the human gait are identified in the Doppler spectrograms. In the next section, we verify this concept using measurement data.

III. Measured Spectrograms of Regular and Anomalous Human Gait Patterns

Measurement data are collected for three different cases using a 2.4GHz Doppler radar testbed in our laboratory [2]. In the first case, the human subject undergoes a regular walking motion for a 6s duration. The subject first walks towards the radar for the first 3s and then turns around and walks away from the radar. The spectrogram, $\chi_{regular}(t,f)$, shown in Fig. 2a., is generated by applying the STFT on the time-domain measurement data using a time window of 0.25s. The spectrogram resembles the spectrogram of a normal human gait generated earlier from simulated data in Fig. 1a. The Doppler resolution is much poorer because of the lower carrier frequency at 2.4GHz when compared to the simulated results at 12GHz. However, the microDopplers arising from the movements of the arms and legs are clearly visible. In the second case, the human subject repeats the same movement while carrying a heavy metal box in his left hand. This results in the left arm and leg not swinging as freely as the right arm and leg. This situation is reflected in the Doppler spectrogram, $\chi_{anomalous1}(t,f)$, shown in Fig. 2b. Next, the human subject repeats the walking motion while carrying a long metallic pole in his left hand. The motion of the human subject carrying this long pole differs significantly from the computer animated motion of the human carrying a metal stick in the previous section. Here, the pole is used like a walking stick. The resulting spectrogram, $\chi_{anomalous2}(t,f)$, is shown in Fig. 2c.

A difference map is generated from $\chi_{regular}(t,f)$ - $\chi_{anomalous1}(t,f)$ and shown in Fig. 2d. The figure focuses on the first 3s of data where the spectrograms in Figs. 1a and b are well aligned along the time axis. Here, we observe some microDoppler features at time instants (0.2 – 0.6)s, (1.2 – 1.7)s and (2.4 – 2.7)s corresponding to the movements of the left arm and leg. The figure clearly indicates the missing microDoppler features from the limited motion of the left limbs in the second measurement case. Next, Fig. 2e is generated from $\chi_{anomalous2}(t,f)$ – $\chi_{regular}(t,f)$. Here, the microDoppler feature from the pole is clearly observed at time instants (0.2 – 0.5)s, (1.4 – 1.5)s and (2.7 – 3)s. The results from Figs. 2d and 2e are qualitatively similar to the findings from the simulation data. Additionally, we generate a difference map from $\chi_{regular}(t,f)$ - $\chi_{anomalous2}(t,f)$. The non-negligible energy observed in Fig. 2f indicates that there are also some missing features in the walking-with-pole data from the normal gait data. This could be due to the shadowing of human body parts by the metal pole. This phenomenon was not observed in the simulation data since the simulation ignored mutual shadowing between body parts.

IV. Conclusion

The spectrograms generated from simulation and measurement data indicate that some anomalies in the human gait can be discerned from the Doppler spectrograms of human gait. Features extracted from the data may be useful for identifying various anomalies which would be useful in situations involving through-wall surveillance.

Acknowledgments

This work is supported by the National Science Foundation under grant CBET-0730924.

References

[1] E. F. Greneker, J. L. Geisheimer, D. S. Andreasen, O. D. Asbel, B. L. Stevens, B. S. Mitchell, "Radar flashlight three years later: An update on developmental progress," *IEEE Annual International Carnahan Conference on Security Technology, Proceedings,* pp. 257 – 259, Oct. 2000.

[2] G. E. Smith, K. Woodbridge and C. J. Baker, "Template based micro-Doppler signature classification," *European Radar Conf.*, pp. 158-161, Sept. 2006.

[3] P. Setlur, M. Amin and F. Ahmad, "Urban target classifications using time-frequency micro-Doppler signatures," *9th Int. Symp. Signal Proc. Its App.*, pp. 1-4, Feb. 2007.

[4] T. Thayaparan, S. Abrol, E. Riseborough, L. Stankovic, D. Lamothe, and G. Duff, "Analysis of radar micro-Doppler signatures from experimental helicopter and human data," *IET Radar Sonar Navig*., vol. 1, pp. 289-299, Aug. 2007.

[5] A. Lin and H. Ling, "A Doppler and direction-of-arrival (DDOA) radar for multiple-mover sensing based on a two-element array," *IEEE Trans. Aerospace Electronic Syst.*, vol. 43, pp. 1496 – 1509, Oct. 2007.

[6] S. S. Ram and H. Ling, "Through wall tracking of humans using joint Doppler and array processing," *IEEE Geoscience Remote Sensing Lett*. vol. 5, pp. 537 – 541, Nov. 2007.

[7] L. M. Frazier, "Surveillance through walls and other opaque materials," *Proc. IEEE National Radar Conference Electronic Systems*, pp. 27 – 31, May 1996.

[8] J. L. Geisheimer, E. F. Greneker and W. S. Marshall, "High-resolution Doppler model of the human gait," *SPIE Proc. Radar Sensor Tech. Data Vis.*, vol. 4744, pp. 8 – 18, July 2002.

[9] V. C. Chen and H. Ling, Time Frequency Transforms for Radar Imaging and Signal Analysis, Artech House, Boston, MA, 2002.

[10] Y.Kim and H. Ling, "Human activity classification based on micro-Doppler signature using artificial neural network," *IEEE Antennas Propagat. Soc. Int. Symp*., July 2008.

[11] S. S. Ram, C. Christianson, Y. Kim and H. Ling, "Simulation and analysis of human microDopplers in through-wall environments," submitted to *IEEE Trans. on Geosc. Remote Sensing*.

[12] S. S. Ram and H. Ling, "Simulation of human microDopplers using computer animation data," *IEEE Radar Conf.*, May 2008.

[13] P. van Dorp and F. C. A. Groen, "Human walking estimation with radar," *IEE Proc. Radar Sonar Navigation*, vol. 150, pp. 356 – 365, Oct. 2003.

[14] J. W. Crispin, Jr. and A. L. Maffett, "Radar cross-section estimation for simple shapes," *Proc. IEEE*, pp. 833 – 848, Aug. 1965.

[15] C. Gabriel, S. Gabriel and E. Corthout, "The dielectric properties of biological tissues. I. Literature Survey," *Phys. Med. Biol.*, vol. 41, pp. 2231 – 2249, 1996.

[16] E. F. Knott, J. F. Shaeffer and M.T.Tuley, Radar Cross Section, Artech House, 2nd Edition, 2004.

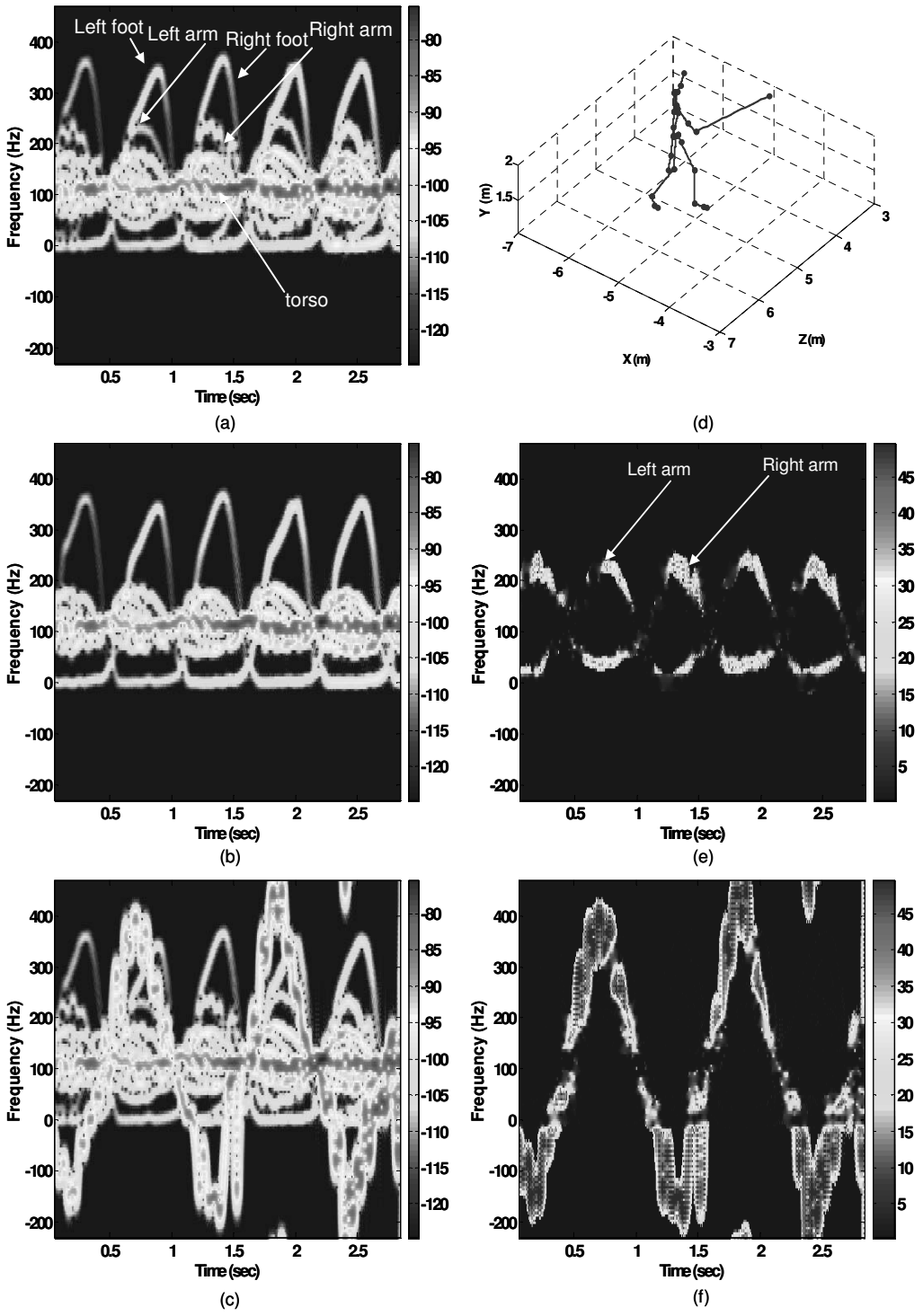

Fig. 1. (a) Simulated spectrogram of regular human gait at 12GHz (high resolution data), $\chi_{regular}(t,f)$.
(b) Simulated spectrogram of human walking without swinging the arms, $\chi_{anomalous1}(t,f)$.
(c) Simulated spectrogram of human walking while carrying a 1.1m metal stick in the left arm, $\chi_{anomalous2}(t,f)$.
(d) Computer animation data of the human carrying the stick used to simulate Fig. 1(c).
(e) $\chi_{regular}(t,f) - \chi_{anomalous1}(t,f)$ shows the missing microDoppler features in Fig. 1(b) due to human arm motions.
(f) $\chi_{anomalous2}(t,f) - \chi_{regular}(t,f)$ shows the additional microDoppler feature in Fig. 1(c) due to the metal stick.

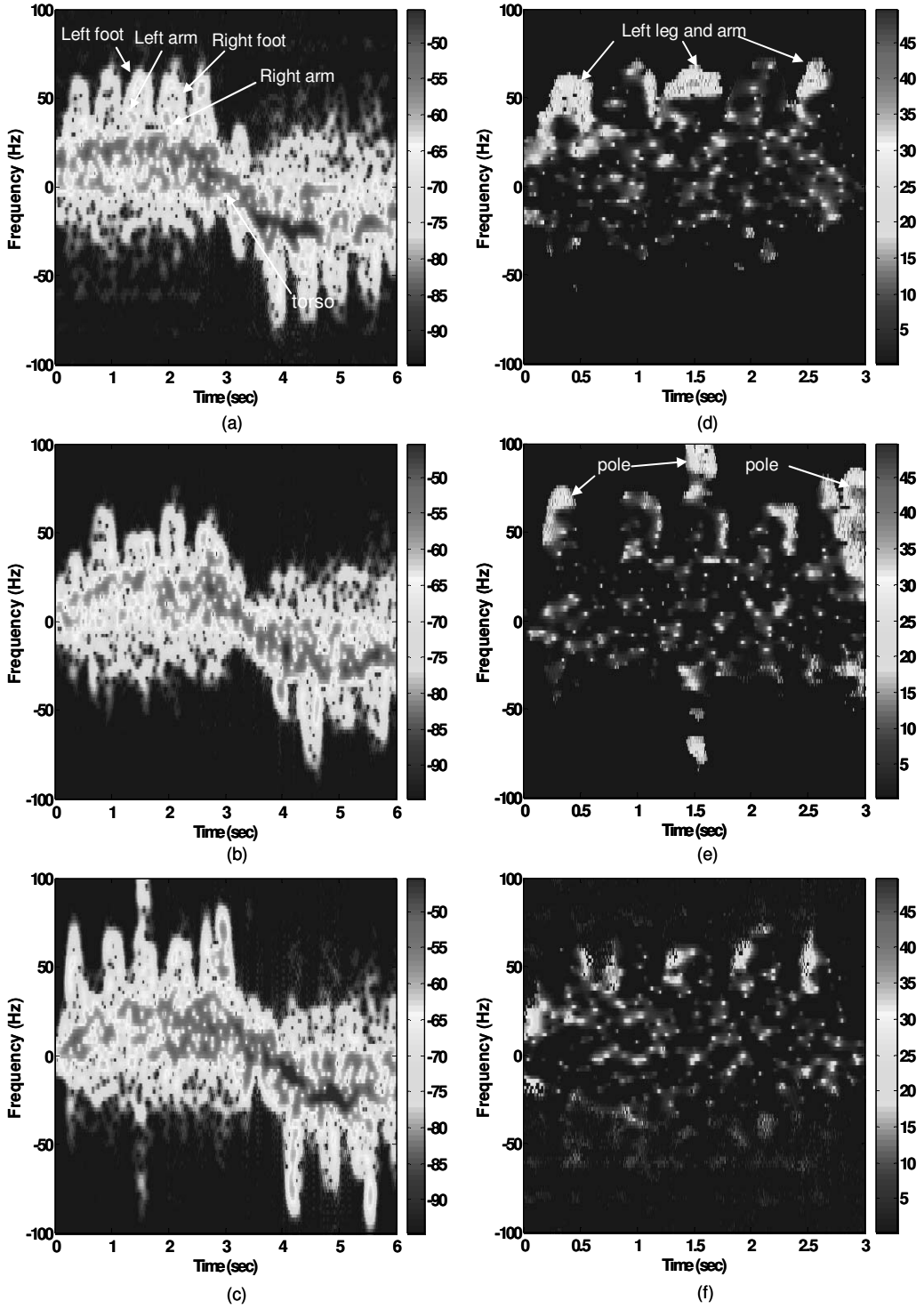

Fig. 2. (a) Measured spectrogram of regular human gait at 2.4GHz (low resolution data), $\chi_{regular}(t,f)$.
(b) Measured spectrogram of human walking while carrying a heavy tool box in the left hand, $\chi_{anomalous1}(t,f)$.
(c) Measured spectrogram of human walking with a long metal pole in the left hand, $\chi_{anomalous2}(t,f)$.
(d) $\chi_{regular}(t,f) - \chi_{anomalous1}(t,f)$ shows the missing microDoppler features in Fig. 2(b) due to motions of the left arm and leg.
(e) $\chi_{anomalous2}(t,f) - \chi_{regular}(t,f)$ shows the additional microDoppler feature in Fig. 2(c) from the metal pole.
(f) $\chi_{regular}(t,f) - \chi_{anomalous2}(t,f)$ shows the missing microDoppler features in Fig. 2(c) due possibly to shadowing by the metal pole.